

See discussions, stats, and author profiles for this publication at: <https://www.researchgate.net/publication/49698772>

# Combined Experimental and Computational Study of Intramolecular Charge Transfer In p-N,N-Dimethylamino-p'-cyano-diphenylacetylene

ARTICLE in THE JOURNAL OF PHYSICAL CHEMISTRY A · FEBRUARY 2011

Impact Factor: 2.69 · DOI: 10.1021/jp109674t · Source: PubMed

CITATIONS

3

READS

56

## 3 AUTHORS:



**Takashige Fujiwara**

The Ohio State University

39 PUBLICATIONS 523 CITATIONS

SEE PROFILE



**Marek Zgierski**

National Research Council Canada

340 PUBLICATIONS 8,215 CITATIONS

SEE PROFILE



**Edward Lim**

University of Akron

99 PUBLICATIONS 1,584 CITATIONS

SEE PROFILE



## NRC Publications Archive Archives des publications du CNRC

**Combined experimental and computational study of intramolecular charge transfer in p-N,N-dimethylamino-p'-cyano-diphenylacetylene**  
Fujiwara, Takashige; Zgierski, Marek Z.; Lim, Edward C.

This publication could be one of several versions: author's original, accepted manuscript or the publisher's version. /  
La version de cette publication peut être l'une des suivantes : la version prépublication de l'auteur, la version acceptée du manuscrit ou la version de l'éditeur.

For the publisher's version, please access the DOI link below. / Pour consulter la version de l'éditeur, utilisez le lien DOI ci-dessous.

### **Publisher's version / Version de l'éditeur:**

<http://dx.doi.org/10.1021/jp109674t>

*Journal of Physical Chemistry A*, 115, 5, pp. 586-592, 2010-12-21

### **NRC Publications Record / Notice d'Archives des publications de CNRC:**

<http://nparc.cisti-icist.nrc-cnrc.gc.ca/npsi/ctrl?action=rtdoc&an=19739612&lang=en>

<http://nparc.cisti-icist.nrc-cnrc.gc.ca/npsi/ctrl?action=rtdoc&an=19739612&lang=fr>

Access and use of this website and the material on it are subject to the Terms and Conditions set forth at

[http://nparc.cisti-icist.nrc-cnrc.gc.ca/npsi/jsp/nparc\\_cp.jsp?lang=en](http://nparc.cisti-icist.nrc-cnrc.gc.ca/npsi/jsp/nparc_cp.jsp?lang=en)

READ THESE TERMS AND CONDITIONS CAREFULLY BEFORE USING THIS WEBSITE.

L'accès à ce site Web et l'utilisation de son contenu sont assujettis aux conditions présentées dans le site

[http://nparc.cisti-icist.nrc-cnrc.gc.ca/npsi/jsp/nparc\\_cp.jsp?lang=fr](http://nparc.cisti-icist.nrc-cnrc.gc.ca/npsi/jsp/nparc_cp.jsp?lang=fr)

LISEZ CES CONDITIONS ATTENTIVEMENT AVANT D'UTILISER CE SITE WEB.

Contact us / Contactez nous: [nparc.cisti@nrc-cnrc.gc.ca](mailto:nparc.cisti@nrc-cnrc.gc.ca).



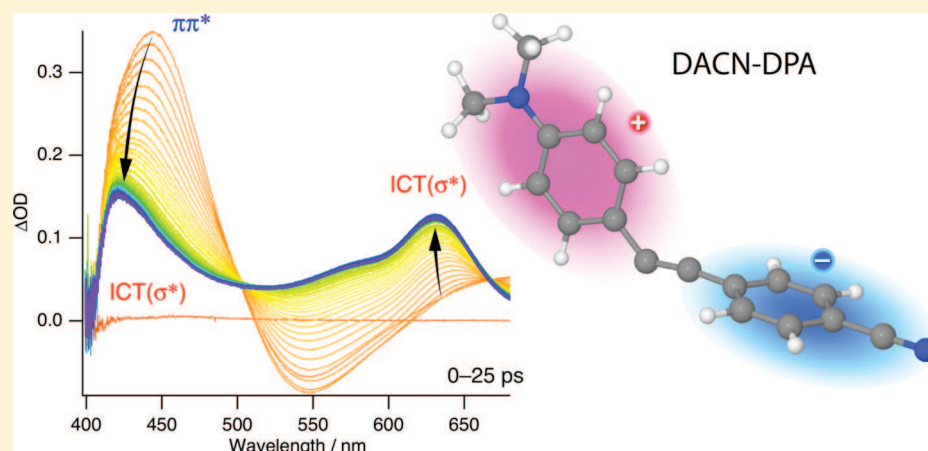
National Research  
Council Canada

Conseil national  
de recherches Canada

Canada

Combined Experimental and Computational Study of Intramolecular Charge Transfer In *p*-*N,N*-Dimethylamino-*p'*-cyano-diphenylacetyleneTakashige Fujiwara,<sup>†</sup> Marek Z. Zgierski,<sup>‡</sup> and Edward C. Lim<sup>\*,†</sup><sup>†</sup>Department of Chemistry and The Center for Laser and Optical Spectroscopy, The University of Akron, Akron, Ohio 44325-3601, United States<sup>‡</sup>Steacie Institute for Molecular Science, National Research Council of Canada, Ottawa, K1A 0R6 Canada

**ABSTRACT:** A concerted experimental (time-resolved spectroscopies) and computational (TDDFT) study of *p*-*N,N*-dimethylamino-*p'*-cyano-diphenylacetylene (DACN-DPA) has been carried out to probe the intramolecular charge transfer (ICT) reaction that occurs in polar solvents. The picosecond transient absorption, as well as fluorescence, in acetonitrile reveals the formation of a twisted ICT( $\sigma^*$ ) state, which involves transfer of an electron from the 4-(dimethylamino)-benzethyne moiety (DMAB) to the benzonitrile (BN) group. This



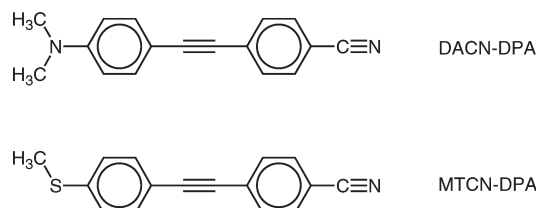
ICT( $\sigma^*$ ) state, with a large dipole moment (24.7 D) and a geometry in which the plane of electron-accepting BN group is perpendicular to the plane electron-donating DMAB moiety and the angles of C(DMAB)C $\equiv$ C is 135.0°, is responsible for the greatly Stokes-shifted ( $\sim 8000\text{ cm}^{-1}$ ) fluorescence and the transient absorption bands (with peaks at about 630 and 425 nm), which decays with the same lifetime ( $\sim 780\text{ ps}$ ). It is proposed that the 630 nm picosecond transient absorption of the ICT state represents the absorption spectrum of dimethylaminobenzethyne radical cation and the 425 nm transient represents the absorption spectrum of benzonitrile radical anion. In nonpolar *n*-hexane, most of the fluorescence as well as the major component of the transient absorption originate from the  $S_1$  ( $\pi\pi^*$ ) state.

## INTRODUCTION

*p*-Methylthio-*p'*-cyano-diphenylacetylene (MTCN-DPA) and *p*-dimethylamino-*p'*-cyano-diphenylacetylene (DACN-DPA), Scheme 1, are classical examples of electron donor–acceptor molecules that exhibit intramolecular charge transfer (ICT) in polar solvents.

The ICT reaction in MTCN-DPA was first reported by Khundker, Stiegman, and Perry,<sup>1</sup> who have shown that the decay rate of ICT fluorescence span both the “normal” and “inverted” regimes of Marcus theory<sup>2</sup> of electron transfer. The ICT state was thought to involve charge transfer reaction from a sulfur nonbonding orbital ( $n_s$ ) to cyano  $\pi$  antibonding orbital ( $\pi_{\text{CN}}^*$ ). The geometries of the ground and the first excited singlet states of MTCN-DPA were calculated by Broo<sup>3</sup> with AM1 method. In polar solvents, the geometry of the ground state is almost planar and the  $\pi$  system is delocalized over the whole molecules. In the excited state, however, the geometry of the two-phenyl rings is perpendicular and the  $\pi$  orbitals are localized on the two-phenyl rings. The excited state is therefore a twisted intramolecular

## Scheme 1



charge transfer (TICT) state.<sup>4</sup> The Stokes shift of the fluorescence spectrum, calculated with a self-consistent reaction field (SCRF) method is  $8220\text{ cm}^{-1}$  in acetonitrile<sup>3</sup> and almost zero in *n*-hexane,<sup>3</sup> which are in agreement with the experimental Stokes

Received: October 8, 2010

Revised: December 7, 2010

Published: December 21, 2010

**Table 1.** TD/B3LYP/cc-pVDZ Vertical Excitation Energies ( $\Delta E$  in eV and nm), Oscillator Strength ( $f$ ), and Orbital Transitions of the Ground State of DACN-DPA at  $C_{2v}$  and  $C_s$  Optimized Geometries

symmetry	excited state	$\Delta E$ (eV)	$f$	transition
$C_{2v}$	$S_1$ ( $2A_1$ )	3.2523 (381.22 nm)	1.0873	$H \rightarrow L$
	$S_2$ ( $1B_2$ )	4.1442 (299.18 nm)	0.0030	$H \rightarrow L + 1$
	$S_3$ ( $2B_2$ )	4.2734 (290.13 nm)	0.0226	$H \rightarrow L + 2$
	$S_4$ ( $3A_1$ )	4.4647 (277.69 nm)	0.3986	$H-1 \rightarrow L, H \rightarrow L + 3$
	$S_5$ ( $1A_2$ )	4.5389 (273.15 nm)	0.0000	$H-3 \rightarrow L$
	$S_6$ ( $3B_2$ )	4.9055 (252.74 nm)	0.0295	$H-2 \rightarrow L$
	$S_7$ ( $4B_2$ )	4.9427 (250.84 nm)	0.0206	$H-4 \rightarrow L, H-1 \rightarrow L + 1$
	$S_8$ ( $4A_1$ )	4.9602 (249.96 nm)	0.0339	$H \rightarrow L + 3$
$C_s$	$S_1$ ( $2A'$ )	3.2574 (380.62 nm)	1.0909	$H \rightarrow L$
	$S_2$ ( $1A''$ )	4.1502 (298.74 nm)	0.0029	$H \rightarrow L + 1$
	$S_3$ ( $2A''$ )	4.2778 (289.83 nm)	0.0219	$H \rightarrow L + 2$
	$S_4$ ( $3A'$ )	4.4657 (277.64 nm)	0.3963	$H-1 \rightarrow L, H \rightarrow L + 3$
	$S_5$ ( $3A''$ )	4.5379 (273.21 nm)	0.000	$H-3 \rightarrow L$
	$S_6$ ( $4A''$ )	4.9054 (252.75 nm)	0.0300	$H-2 \rightarrow L$
	$S_7$ ( $5A''$ )	4.9439 (250.78 nm)	0.0211	$H-4 \rightarrow L, H-1 \rightarrow L + 1$
	$S_8$ ( $4A'$ )	4.9604 (249.95 nm)	0.0338	$H \rightarrow L + 3$

shifts ( $8145\text{ cm}^{-1}$  in acetonitrile and  $2600\text{ cm}^{-1}$  in *n*-hexane).<sup>1</sup> Although these results are consistent with the occurrence of an ICT reaction in photoexcited MTCN-DPA, the mechanism of the ICT process remains unclear due to the absence of time-resolved transient absorption data for the molecule.

The ICT reaction of DACN-DPA in various solvents has been studied by Hirata, Okada, and Nomoto,<sup>5</sup> using time-resolved fluorescence and transient absorption techniques. In *n*-hexane, the transient absorption has a strong peak at 510 nm and weaker bands at 600 and 710 nm. All three transients decay with a lifetime of about 650 ps, which is the same as the rise time of triplet state absorption ( $T_n \leftarrow T_1$ ). The results indicate that the 510, 600, and 710 nm transients are the excited-state absorption spectra of the lowest excited singlet state (the locally excited, LE state). Consistent with this conclusion, the lifetime ( $\sim 650$  ps) of the picosecond transients is essentially identical to the 660 ps decay time of LE fluorescence in *n*-hexane. In 1-butanol, the weak fluorescence at about 410 nm, attributed to the emission from the LE state, appears together with the strong ICT fluorescence at about 570 nm. The 410 nm emission has decay time of about 20 ps, whereas the 570 nm emission exhibits a short rise time ( $\sim 20$  ps) and a long decay time ( $\sim 480$  ps at 650 nm). The picosecond time-resolved absorption spectra of DACN-DPA in 1-butanol is composed of the transient at 490 nm, with a decay time of about 20 ps, and two transients at about 430 and 690 nm, with a decay time of about 460 ps. The correspondence between the decay time of the 570 nm ICT fluorescence and that of the 430 and 690 nm transients led Hirata et al.<sup>5</sup> to conclude that these transients are the excited-state absorption spectra of the ICT state. In acetonitrile, the picosecond absorption appears at about 630 and 405 nm. Although the formation time of these transients, with a decay time of subnanosecond, is too fast to be measured with the time resolution (tens of picoseconds) of their experiment, the 630 and 405 nm transients have been assigned to the absorption spectra of the ICT state.

To characterize the electronic states and reaction pathway of ICT reaction, it is essential to carry out time-resolved fluorescence and transient absorption experiments with greater time-resolution and compare them with quantum mechanical calculations of the electronic states and electronic spectra. In this paper,

**Table 2.** TD/B3LYP/cc-pVDZ Adiabatic Energies ( $\Delta E$ ), Emission Energies ( $E_{\text{ems}}$ ), Oscillator Strengths ( $f$ ), and Dipole Moments ( $|\mu|$ ) for the Five Low-Energy Excited Singlet States of DACN-DPA

state	$\Delta E^a$ (kcal/mol)	$E_{\text{ems}}$ (eV)	$f$	$ \mu $ (D)
$\pi\sigma^*$	0.00	1.346 (921 nm)	0.0006	13.89
$\pi\pi^*$	−0.62	3.131 (396 nm)	1.1827	21.22
ICT	−4.10	2.276 (545 nm)	0.00000	28.96
ICT(p)	−7.57	2.644 (469 nm)	0.0000	29.96
ICT( $\sigma^*$ )	−10.24	1.884 (658 nm)	0.00006	24.74

<sup>a</sup> Adiabatic minimum energy relative to the highest  $\pi\sigma^*$  state (−765.12027825 au).

we present a concerted experimental and computational study of ICT reaction in the photoexcited DACN-DPA.

## METHODS

The time-resolved excited-state absorption spectra were measured using the Ti:sapphire-based transient absorption setup described in refs 6 and 7. Briefly, the subpicosecond pump–probe experiments were carried out using  $\sim 100$  fs pump pulses with a center wavelength of 315 nm from an optical parametric amplifier (Light Conversion, TOPAS), which was pumped by the fundamental (800 nm) of the Ti:sapphire regenerative amplifier (Quantronix, Titan). A weak fundamental beam of the regenerative amplifier traveling through a variable delay stage (Newport, IMS600CCHA) was focused onto a  $\text{CaF}_2$  plate to generate a probe white light continuum (310–750 nm). The probe pulse was then focused to the sample solution in a flow cell (1.0 mm thickness) and intersected the pump beam with a narrow crossed angle ( $<3^\circ$ ). We installed a linear motion of the cell implemented via a crank mechanism to make its surfaces periodically changed during irradiation of the UV-pump beam. It helped to prevent photopolymerized sample adsorbing onto the inner cell surface, especially in *n*-hexane solution. The time-resolved transient absorption (TA) spectra were mapped out as a function of delay time between the pump and probe pulses, using a CCD detector (PI, PIXIS 400B) attached to a spectrograph

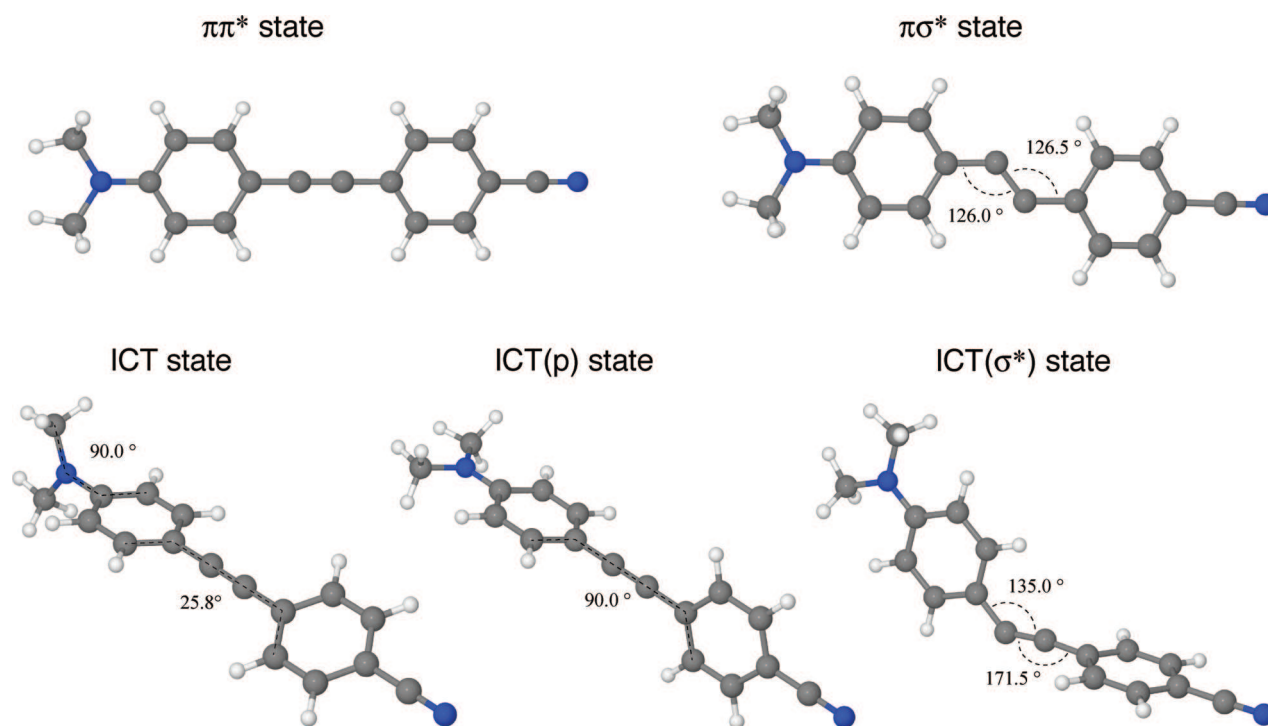


**Figure 1.** TD/B2LYP/cc-pVDZ optimized geometries of the five excited singlet states of DACN-DPA.

(Acton, Spectra Pro 2300i). Temporal decay profiles at specific wavelengths were extracted from the mapped TA spectra and analyzed by deconvolution procedures with nonlinear least-squares fittings.

Picosecond time-resolved fluorescence spectrum (TR-FS) was obtained by an optical Kerr-gating technique to skim an emission spectrum as a function of the delay time, as described in ref 8. Benzene as Kerr medium was filled in a static cell (1 mm thickness) and placed between two thin high-contrast polarizers (Moxtek, ProFlux PFU05C) at crossed polarization configuration. The excitation beam was focused onto the sample in the flow cell and its emission was collected collinearly along the pump beam, and imaged onto the Kerr cell via two parabolic reflectors. The gating pulse (800 nm, <100 μJ) was traveling through a variable delay stage (Newport, IMS600CCHA) and focused to the Kerr cell, where the emission and the gate pulse spatially overlapped each other to drive the Kerr shutter open at a given delay time. The typical temporal resolution was estimated as ~1 ps for the Kerr gating. Finally, the gated fluorescence was introduced to a polygraph spectrometer (Acton, Spectra Pro 2300i) attached to a CCD detector (PI, PIXIS 400B) to create the spectrum. Temporal decay profiles at specific wavelengths were extracted from the mapped spectra and analyzed by deconvolution procedures with nonlinear least-squares fitting.

DACN-DPA, synthesized by Ms. Tia Walker, was the gift of Professor Yi Pang of The University of Akron. The compound was determined to be greater than 99.5% pure by GC/MS and NMR. The steady-state UV absorption and fluorescence spectra were measured by using a UV spectrophotometer (Shimadzu; UV-1800) and a spectrofluorometer (Horiba/Jobin Yvon; FluoroMax-4), respectively. Spectral corrections for the fluorescence spectra were made for correct spectral profile.

The time-dependent DFT (TDDFT) calculations of the excitation energies and oscillator strengths of the excited-state

**Table 3.** Comparison of TD/B3LYP/cc-pVDZ Excited-State Absorption Spectra of the ICT( $\sigma^*$ ) State of DACN-DPA with Experiment

transition	$\Delta E$ (eV)	$f$	expt <sup>a</sup> (nm)
$S_6 \leftarrow S_1$	1.859 (667.0 nm)	0.9235	640
$S_9 \leftarrow S_1$	2.714 (456.8 nm)	0.7782	425

<sup>a</sup> The transient absorption spectra of DACN-DPA in acetonitrile.

absorptions were performed using TURBOMOLE suite of programs<sup>9</sup> with B3LYP and BP86 functionals and cc-pVDZ basis set. The geometries of the excited  $S_1$  ( $n\pi^*$ ) and  $S_2$  ( $\pi\pi^*$ ) states were optimized at the TD/B3LYP level.

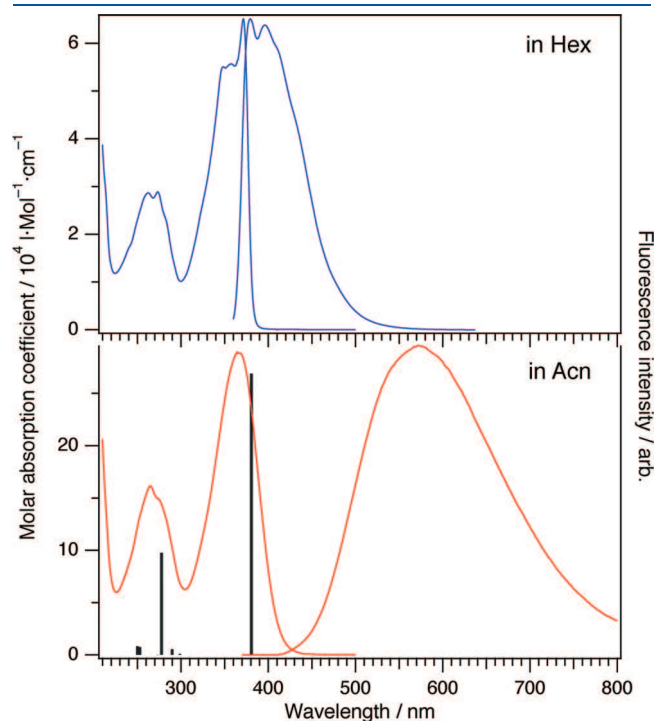
## RESULTS AND DISCUSSION

Table 1 presents the vertical B3LYP/cc-pVDZ excitation energies, and oscillator strength ( $f$ ), of the ground state of DACN-DPA at  $C_{2v}$  and  $C_s$  geometries. The  $C_s$  symmetry arises from the relaxation of the  $C_{2v}$  symmetry, which leads to pyramidalization of the dimethylamino (DMA) group. This is the lowest minimum of the  $S_0$  potential energy surface, with the DMA pyramidalization angle of 5.3 degrees and mode frequency of 57  $\text{cm}^{-1}$ . The calculations predict two highly allowed transitions for the molecule at the  $C_{2v}$  and  $C_s$  geometries. These are  $S_1 \leftarrow S_0$  absorption and  $S_4 \leftarrow S_0$  absorption at 381 nm ( $f = 1.09$ ) and 278 nm ( $f = 0.40$ ). These predictions are in excellent accord with the experimental absorption bands at about 370 and 270 nm (*vide infra*). The  $S_1 \leftarrow S_0$  absorption is of HOMO (highest occupied molecular orbital)  $\rightarrow$  LUMO (lowest unoccupied molecular orbital), whereas the  $S_4 \leftarrow S_0$  absorption is of  $H - 1 \rightarrow L$  and  $H \rightarrow L + 3$  combination.

The TD/B3LYP/cc-pVDZ calculations yield five excited singlet states of similar energies for DACN-DPA. These are  $\pi\pi^*$ ,  $\pi\sigma^*$ , ICT, ICT(p), and ICT( $\sigma^*$ ) state, in the order of decreasing



energies. The adiabatic energies, oscillator strengths, and the dipole moments of the five excited states are summarized in Table 2. The computed TD/B3LYP/cc-pVDZ geometries of the



**Figure 2.** Steady-state absorption/emission spectra of DACN-DPA in *n*-hexane and acetonitrile at room temperature. The ground-state absorption (stick) spectrum with computed (TDDFT) vertical excitation energy with oscillator strength is also shown for comparison (see Table 1).

five excited states are also given in Figure 1. In the lowest energy ICT( $\sigma^*$ ) state, an electron is transferred from the dimethylaminobenzene (DMAB) moiety to the benzonitrile (BN) group. The plane of C(DMAB)CC is perpendicular to the plane of BN group. The dipole moment of the state is 24.7 D, with angles of C(DMAB)CC = 135.0° and C(BN)CC = 171.5°. The symbol  $\sigma^*$  in the parentheses is used to indicate the fact that the carbon atom in the C $\equiv$ C moiety, next to DMAB, is distorted by an angle of 135°. The 90° rotation of the BN plane, relative to the rest of the molecule, in the ICT( $\sigma^*$ ) state of DACN-DPA is similar to the AM1 excited state geometry of MTCN-DPA, calculated by Broo.<sup>3</sup> The TD/B3LYP/cc-pVDZ transient absorption spectra of the ICT( $\sigma^*$ ) state are shown in Table 3. The calculation yields two allowed  $S_n \leftarrow S_1$  ICT( $\sigma^*$ ) transitions at about 457 nm ( $f = 0.78$ ) and at about 667 nm ( $f = 0.92$ ), which agree very well with the experimental picosecond transient absorption spectra (vide infra).

In the ICT state, the dimethylamino group is twisted 90° with respect to the planar benzethyne (BE) and the BN moieties. Here, the electron donor is the dimethylamino group and the electron acceptor is the rest of the DACN-DPA moieties. The dipole moment of the ICT state is 29.0 D and the extremely weak transition ( $f \sim 10^{-5}$ ) to the ground state is expected to occur at about 545 nm. The ICT( $\sigma^*$ ) state differs from the ICT(p) state (the “p” in parentheses stands for “perpendicular”) in that the two ring planes are perpendicular, with a straight C(DMAB)CCC (BN line), and the dimethylamino group is in the ring plane of DMAB moiety. The  $\pi\pi^*$  state, which is strongly allowed ( $f = 1.18$ ) from the ground state, has the dipole moment of 21.2 D, Table 2. The adiabatic minimum of the  $\pi\pi^*$  state (396 nm) is in excellent agreement with the emission maximum of the fluorescence in *n*-hexane (vide infra). Finally, the  $\pi\sigma^*$  state is the planar excited state that arises from the promotion of an electron from the  $\pi$

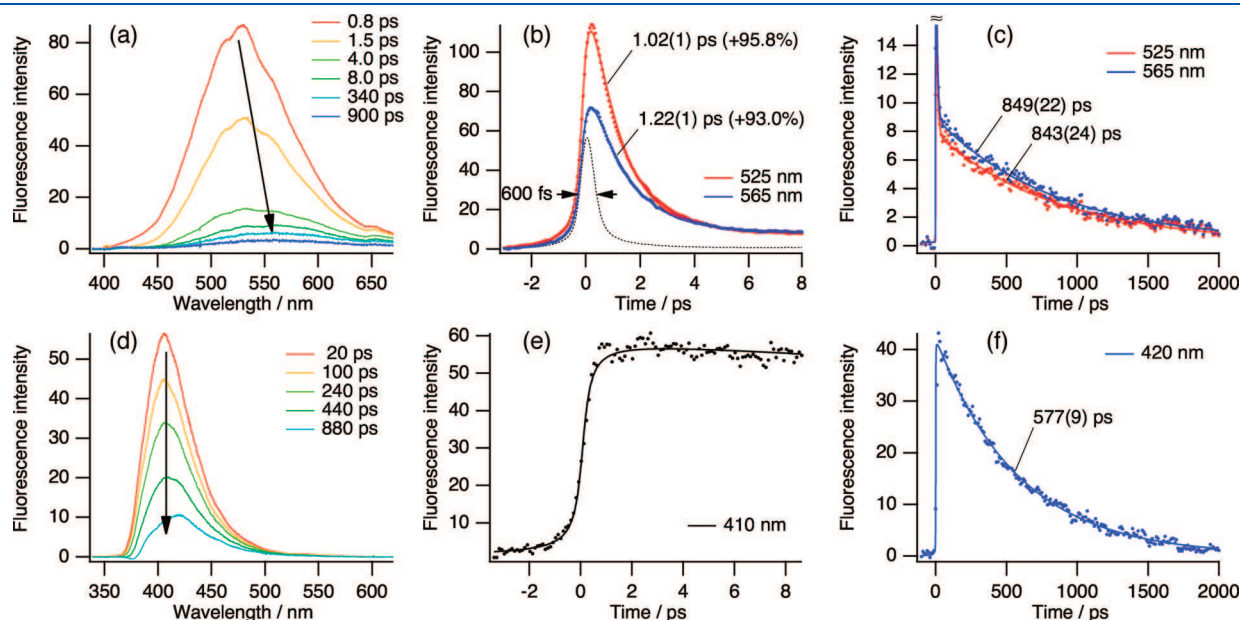


**Figure 3.** Picosecond time-resolved fluorescence spectra (TR-FS) and the temporal profiles of DACN-DPA in acetonitrile (upper panels) and in *n*-hexane (lower) at room temperature, obtained by the optical Kerr-gating technique (see more details in text). The TR-FS of DACN-DPA (a) in Acn and (d) in Hex were chirp-corrected and arrows indicate time evolutions of the spectra together with its band shift. The fluorescence decay curves at a specific center wavelength were generated with band integration of the time-resolved fluorescence. The system response was estimated to be about 600 fs (fwhm) from a solvent Raman signal as inset in (b; dash curve). The decay time constants were evaluated by a nonlinear least-squares fit with deconvolution procedure. The numbers in the parentheses indicate a standard deviation ( $1\sigma$ ).

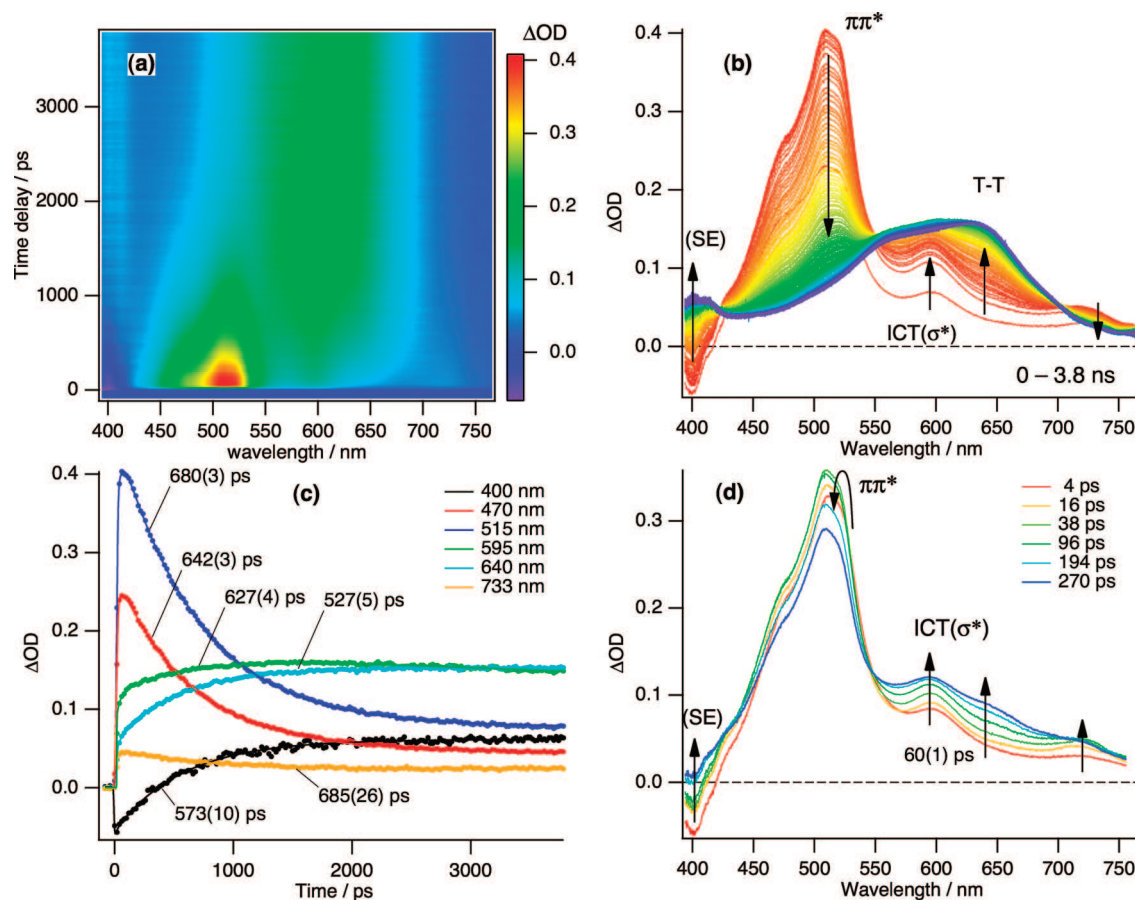


**Figure 4.** Femtosecond time-resolved transient absorption spectra (TAS) and the temporal profiles of the excited-state DACN-DPA in *n*-hexane at room temperature ( $\lambda_{\text{exc}} = 340$  nm): (a) 2-D image plot and (b) its corresponding time-evolved spectra in the long time range (0–3.8 ns with an interval of 20 ps). Arrows indicate the time-evolution of the spectra, and assignments are also shown for the transients;  $\pi\pi^*$ , ICT( $\sigma^*$ ), and stimulated emission (SE). (c) Kinetics at the transients of interest, which were extracted with a band integration from the 2-D plot (a) along time. Leaders show the fitted decay times with a standard deviation in the parentheses. (d) Time-resolved TAS shows the earlier spectral time-evolution.

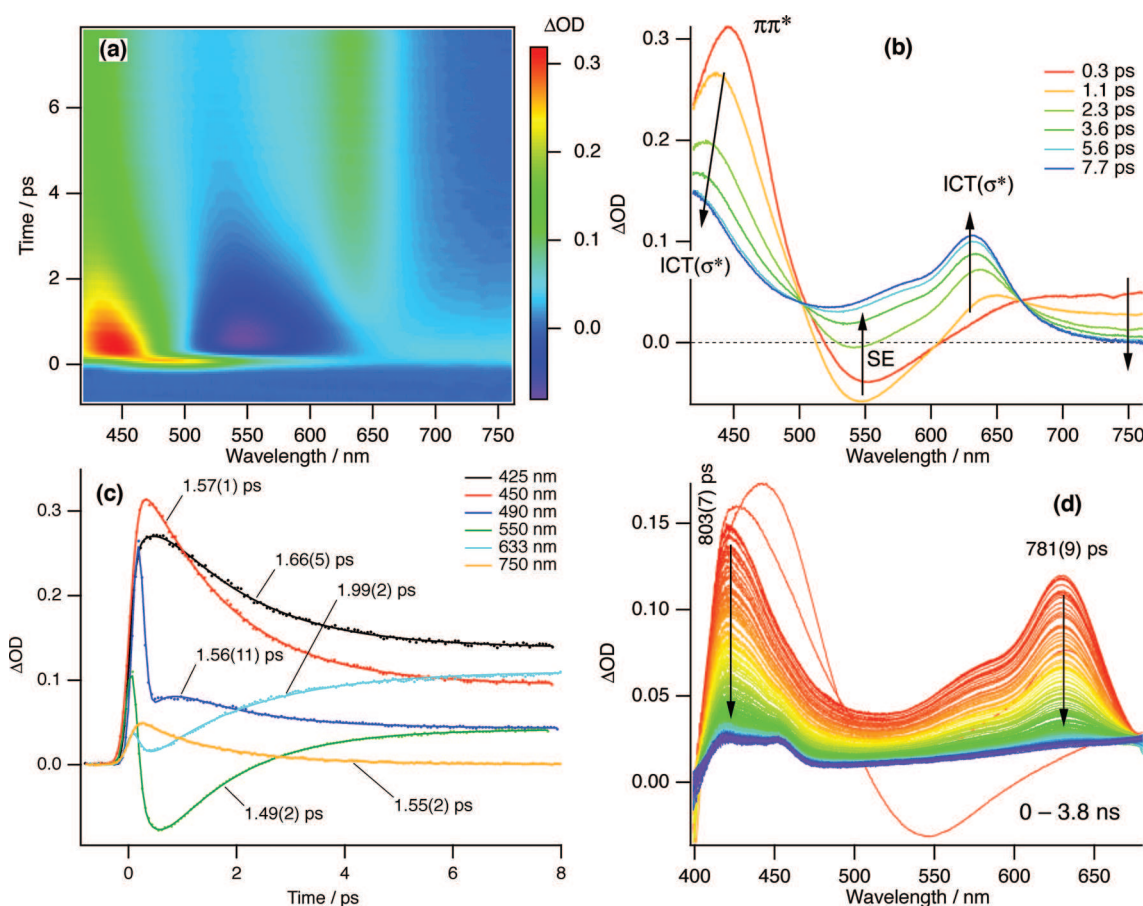
orbital to the  $\sigma^*$  orbital, which is localized on the acetylenic bond. The  $\pi\sigma^*$  state has similar C(DMAB)CC and C(BN)CC angles and the smallest dipole moment (13.89 D) of the five excited singlet states of DACN-DPA.

Figure 2 presents the steady-state absorption and fluorescence spectra of DACN-DPA in *n*-hexane and acetonitrile at room temperature. The strong absorption band at about 370 nm and the weaker absorption band at about 270 nm are in very good agreement with the computed  $\pi^* \leftarrow \pi$  vertical excitation energies of the ground state at about 381 nm ( $S_1 \leftarrow S_0$ ,  $f = 1.09$ ) and at about 278 nm ( $S_4 \leftarrow S_1$ ,  $f = 0.40$ ), Table 1. The strong red shift of the fluorescence in acetonitrile (and the very small spectral overlap with the  $S_1 \leftarrow S_0$  absorption band), relative to *n*-hexane, indicates that the fluorescence of the compound in acetonitrile originates from a highly polar excited state. The temporal decay profile of the time-resolved fluorescence spectrum is biexponential, as shown in Figure 3a–c. The ultrafast (<1 ps) decay is followed by the slower 849 ps decay. The presence of the ultrafast decay component with the slight spectral band-shift suggests that the occurrence of a very fast transformation of the initially excited state along with solvation to the state which gives rise to the slow ( $\sim 850$  ps) emission. In *n*-hexane, the fluorescence spectrum is a good mirror image of the  $S_1(\pi\pi^*) \leftarrow S_0$  absorption, and it can be assigned to the emission from the  $S_1(\pi\pi^*)$  state. The temporal profile in *n*-hexane shows a single

exponential decay of  $\sim 577$  ps without any ultrafast decay involved, Figure 3d–f.

Figure 4a–d shows the femtosecond time-resolved transient absorption (TA) spectra of DACN-DPA in *n*-hexane, measured at a 340 nm excitation of the molecule at room temperature. The observed excited-state absorption in a longer time range, Figure 4b, has two major features in the spectral range of 400–750 nm. The first is a band at about 515 nm, which decays with lifetime of about 680 ps, and the second is the bands at about 595 and 640 nm, which rise in about 560 ps. The close agreement between the decay times of the 515 nm transient with the rise time of the 595/640 nm transients as well as an existence of isosbestic points at 422, 550, and 703 nm indicates that the 595/640 nm transients are formed from the state responsible for the 515 nm transient in the long time range (0–3.8 ns). Furthermore, from the observation of the 595/640 nm transients staying positive in the course of delay time, the majority of band contribution may be a triplet  $\rightarrow$  triplet ( $T_1 \rightarrow T_n$ ) absorption, which can be seen as terminal states in common for most of ICT molecules.

Comparison with the computed vertical excitation energies of the five low-lying excited states indicates that the 595/640 nm transients are the  $S_9 \leftarrow S_1$  and  $S_6 \leftarrow S_1$  transients of the ICT( $\sigma^*$ ) state, which are predicted to occur at about 457 nm ( $f = 0.78$ ) and 667 nm ( $f = 0.92$ ) in vacuo, respectively. The TD/B3LYP/cc-pVDZ vertical excitation energies of other excited states



**Figure 5.** Femtosecond time-resolved transient absorption spectra (TAS) and the temporal profiles of the excited-state DACN-DPA in acetonitrile at room temperature ( $\lambda_{\text{exc}} = 340$  nm): (a) chirp-corrected 2-D image plot (wavelength vs delay time) and (b) its corresponding time-evolved spectra in the long time range (0–3.8 ns with an interval of 20 ps). Arrows indicate the time evolution of the spectra, and assignments are also shown for the transients;  $\pi\pi^*$ , ICT( $\sigma^*$ ), and stimulated emission (SE). (c) The earlier temporal profiles of the transients, which were extracted with a band integration from the 2-D plot (a). The intense spike at time zero for 490 and 550 nm transients is due to the coherent signal from an acetonitrile solvent that was also included in the overall fit for removal. Leaders show the fitted decay times with a standard deviation in the parentheses. (d) Time-resolved TAS shows the spectral time-evolution at the later time range (0–3.8 ns with an interval of 20 ps).

(Table 2) do not agree with the experimental spectra at all. On the basis of these observations, we assign the 515 nm transient to the absorption spectrum of the  $S_1$  ( $\pi\pi^*$ ) state and the 595/640 nm transients to the ICT( $\sigma^*$ ) state. Consistent with the assignment of the 515 nm absorption to the  $S_1$  ( $\pi\pi^*$ ) state, its decay time of  $\sim 580$  ps for the transient agrees with the 577 ps decay time of fluorescence, Figure 3f.

In TAS of the earlier time profiles of DACN-DPA in *n*-hexane, as shown in Figure 4d, a very fast rise component of  $\sim 1$  ps can be found at 515/640 nm absorption, followed by a slow rise of around 50–60 ps, whereas the main 515 nm transient for  $S_1$  ( $\pi\pi^*$ ) state shows the similar behavior to those at 515/640 nm absorption, but decays with a time constant of about 580 ps, which is consistent with recovery time of 573 ps of the stimulated emission (SE) in TA spectra.

The time-resolved TA spectra of DACN-DPA in acetonitrile are given in Figure 5a–d. At a pump–probe delay time of 0.3 ps, there appears a transient absorption with intensity maxima at about 450 nm. This subpicosecond TA resembles the 515 nm  $\pi\pi^*$  state absorption spectrum of DACN-DPA in *n*-hexane. As the 450 nm disappears, the transients at about 425 and 630 nm, very similar to the spectra in *n*-hexane, appear for pump–probe delay times longer than a few picoseconds. The ultrafast ( $\sim 1.5$  ps)

decay time of the initially excited  $\pi\pi^*$  transient at about 450 nm is consistent with the ultrafast ( $\sim 1$  ps) decay time of the time-resolved fluorescence, given in Figure 3b. The slow decay time ( $\sim 800$  ps) of the 425/630 nm transients in Figure 5d, agree with the decay time of  $\sim 850$  ps decay time of fluorescence in Figure 3c, indicating that both the greatly Stokes-shifted fluorescence as well as the 425/630 nm transients originate from the ICT( $\sigma^*$ ) state. The assignments of the 425/630 nm transients to the ICT( $\sigma^*$ ) state, which involves a charge transfer from the dimethylaminobenzethyne (DMABE) group to the benzonitrile (BN) moiety, is supported by the fact that the 630 nm transient closely resembles the absorption spectrum of DMABE positive ion, and the 425 nm transient closely mimics the absorption spectrum of benzonitrile anion.<sup>10</sup> It is pertinent to note that the  $\pi\pi^* \rightarrow$  ICT( $\sigma^*$ ) transition is about 2 orders of magnitude faster in acetonitrile (a few picosecond) than in *n*-hexane ( $\sim 680$  ps), consistent with the strong solvent-polarity dependence of the barrier for the ICT( $\sigma^*$ ) state formation.

## CONCLUSION

We have carried out time-resolved fluorescence and transient absorption studies, and TDDFT calculations, of the low-lying excited states of *p*-*N,N*-dimethylamino-*p'*-cyano diphenylacetylene



(DCN-DPA), for the purpose of probing the mechanism of excited-state intramolecular charge transfer. In polar acetonitrile, the fluorescence as well as the transient absorption (TA) reveals the formation of an ICT state, which arises from the transfer of an electron from the dimethylaminobenzethyne (DMABE) group to the benzonitrile (BN) moiety. The TDDFT calculations as well as the time-resolved spectral studies are consistent with the conclusion that the ICT state, with a very large dipole moment (24.7 D), has the plane of DMABE group that lies perpendicular to the plane of the BN group. The lifetime of the ICT state transient is identical to the decay time of fluorescence from the  $S_1$  ( $\pi\pi^*$ ) state. In nonpolar *n*-hexane, the transient absorption due to the ICT state also appears, but its formation time is quite slow ( $\sim 680$  ps), and most of the fluorescence as well as the major component of the transient absorption, originate from the  $S_1$  ( $\pi\pi^*$ ) state of the molecule.

## AUTHOR INFORMATION

### Corresponding Author

\*E-mail: elim@uakron.edu.

## ACKNOWLEDGMENT

We are very grateful to Ms. T. Walker and Prof. Y. Pang at the University of Akron for the synthesis of DACN-DPA.

## REFERENCES

- (1) Khundkar, L. R.; Stiegman, A. E.; Perry, J. W. *J. Phys. Chem.* **1990**, 94, 1224.
- (2) Marcus, R. A. *J. Chem. Phys.* **1965**, 43, 679.
- (3) Broo, A. *Chem. Phys.* **1994**, 183, 85.
- (4) Grabowski, Z. R.; Rotkiewicz, K.; Rettig, W. *Chem. Rev.* **2003**, 103, 3899 and references therein.
- (5) Hirata, Y.; Okada, T.; Nomoto, T. *Chem. Phys. Lett.* **1997**, 278, 133.
- (6) Lee, J.-K.; Fujiwara, T.; Kofron, W. G.; Zgierski, M. Z.; Lim, E. C. *J. Chem. Phys.* **2008**, 128, 164512.
- (7) Fujiwara, T.; Lee, J.-K.; Zgierski, M. Z.; Lim, E. C. *Chem. Phys. Lett.* **2009**, 481, 78.
- (8) Zgierski, M. Z.; Fujiwara, T.; Lim, E. C. *J. Chem. Phys.* **2010**, submitted for publication.
- (9) Ahlrichs, R.; Bär, M.; Häser, M.; Horn, H.; Kölmel, C. *Chem. Phys. Lett.* **1989**, 162, 165.
- (10) Zgierski, M. Z.; Lim, E. C. *Chem. Phys. Lett.* **2004**, 393, 143.